Desalination and Water Treatment
www.deswater.com
doi: 10.1080/19443994.2015.1135481

57 (2016) 23651–23660
October

Taylor & Francis
Taylor & Francis Group

Sea water vapor pressure based on the Cisternas–Lam model

Luis A. Cisternas[a,b,*], Renato Acosta-Flores[a,b], Višnja Musič[a]

[a]*Departamento de Ingeniería Química y Procesos de Minerales, Universidad de Antofagasta, Antofagasta, Chile, emails: luis.cisternas@uantof.cl (L.A. Cisternas), renato.acosta@ua.cl (R. Acosta-Flores), bisnja@hotmail.com (V. Musič)*
[b]*Centro de Investigación Científico Tecnológico para la Minería, CICITEM, Antofagasta, Chile*

Received 25 September 2015; Accepted 18 December 2015

ABSTRACT

The values of sea water vapor pressure (SWVP) and boiling point elevation (BPE) are required in the simulation, design, and optimization of processes in which sea water is used, such as in the mining industry and in a desalination plant. The SWVP is modeled using the model of Cisternas and Lam (CL). The literature on SWVP is reviewed, and several models and SWVP data are selected to assess the CL model using other models that are available in the literature. Two cases are analyzed in the application of CL model: first, the sea water is modeled as a mixture of salt with fixed ionic strength fraction and the capability of CL model to predict the SWVP is analyzed; next, as the second-best option, the sea water is modeled as a pseudo 1:1 electrolyte, which requires a single empirical constant to be set. The CL model is assessed using several models. Two sets of experimental data are used to study the capability of the SWVP models regarding their interpolation, extrapolation, and correlation of the data. The CL model usually gives the best results in terms of the interpolation, extrapolation and correlation of the SWVP. In addition, the application of the CL model to estimate the BPE is shown. An accuracy of 0.03 K was observed in the prediction of the BPE.

Keywords: Sea water; Vapor pressure; Boiling point elevation

1. Introduction

Water is the basic natural resource for both the development of human society and the survival of ecosystems. Population growth, ongoing industrialization, and the need to increase agricultural production all increase the stress on this vital resource; water has thus become a bottleneck for the sustainable development of increasing numbers of countries and regions. For example, in the Antofagasta region (Chile), water scarcity is one of the main problems for the mining industry, whether for mine expansion, the exploitation of existing mines or the development of new mines. Antofagasta is located in the Atacama Desert, which is commonly known as the driest place in the world. Given this lack of water, the use of sea water has become the most appropriate method for obtaining water. Thus, several desalination plants based on reverse osmosis have been installed to provide drinking and industrial water. As a result, most of the new mining projects have considered and continue to include the use of sea water or desalinated water to supply their operations.

The properties of sea water have become important information for the development of these processes. Sharqawy et al. [1] reviewed the correlations and data

*Corresponding author.

for the thermophysical properties of sea water. These properties included density, specific heat capacity, thermal conductivity, dynamic viscosity, surface tension, vapor pressure, boiling point elevation (BPE), latent heat of vaporization, specific enthalpy, specific entropy, and osmotic coefficient. They made comparisons among the correlations and provided recommendations for each property, particularly over the ranges of temperature and salinity that are common in thermal and/or reverse osmosis sea water desalination applications. Most of the correlations analyzed were empirical, typically polynomial functions, with many parameters. Note that polynomial models have poor interpolation and extrapolation properties. In addition, polynomial models primarily exhibit a poor trade-off between shape and degree. To model data with a complex behavior, the model degree must be high, which means that the associated number of parameters to be estimated will also be high. This can result in highly unstable models. Recently, artificial neural networks were applied to correlate and predict the physicochemical, transport, and thermodynamic properties of sea water [2]. The artificial neural networks model obtained provided lower deviations than did other, more sophisticated models presented in the literature, with absolute deviations lower than 0.5%. Although neural networks offer a number of advantages, their "black box" nature, greater computational burden, proneness to over fitting, and the empirical nature of the model development are the main drawbacks [3]. In addition, Pade´ approximants were used to model the physicochemical, transport, and thermodynamic properties of sea water for industrial applications [4]. The general models obtained were of rational type and resulted in deviations similar to those provided by the more sophisticated models presented in the literature, but with fewer parameters. However, the empirical nature of the model development is the main drawback of this work.

A summation of SWVP empirical models is given in Table 1. The models are found to be valid only in a limited range of temperature and salinity. These models require more than five fitting parameters or experimental values of water vapor pressure. The sea water properties can also be modeled using thermodynamic models. For example, the specific Gibbs energy of sea water can be used to model the heat capacities, freezing points, and vapor pressures [9]. However, these models are more complex and can be very demanding for application in the optimization and design problems. In addition, Cisternas and Lam [10] compared their model results with the thermodynamic models of Pitzer and Bromley and found that the CL model gives better results, with 1/2–1/12 of the errors obtained for these methods. The objective of this work is to show that the semi-empirical model of CL [11] can be used to model both the sea water vapor pressure (SWVP) and the BPE.

2. Cisternas and Lam model

Cisternas and Lam [11] developed a model of the vapor pressure over electrolyte solutions based on a single empirical constant for each electrolyte. The method is based on the Kumar–Patwardhan procedure to estimate the vapor pressure [12,13]. Cisternas and Lam presented the following equation:

$$\log_{10} P = K I \left[A - \frac{B}{T - E_s}\right] + \left[C - \frac{D}{T - E_s}\right] \tag{1}$$

$$A = A_s + 3.60591 \times 10^{-4} I + M_s/2303 \tag{2}$$

$$B = B_s + 1.382982 I - 0.031185 I^2 \tag{3}$$

$$C = C_s - 3.99334 \times 10^{-3} I - 1.11614 \times 10^{-4} I^2 + M_s I (1 - \chi)/2303 \tag{4}$$

$$D = D_s - 0.138481 I + 0.07511 I^2 - 1.79277 \times 10^{-3} I^3 \tag{5}$$

$$\chi = 2(\upsilon_+ + \upsilon_-)/(\upsilon_+ Z_+^2 + \upsilon_- Z_-^2) \tag{6}$$

where P is the vapor pressure (kPa), T is the temperature (K), I is the ionic strength (mol kg^{-1}), M_s is the molecular weight of the solvent, K is an electrolyte parameter, and A_s, B_s, C_s, D_s, and E_s are solvent parameters. In Eq. (6), υ_+ is the number of moles of cations, υ_- is the number of moles of anions produced by the dissociation of one mole of the electrolyte, Z_+ denotes the valence of the cation, and Z_- denotes the valence of the anion. Therefore, the model has six parameters, one parameter for each salt (K) and five parameters for each solvent (A_s, B_s, C_s, D_s, and E_s). The K values of 111 single electrolytes and solvent constants for 5 solvents were reported by Cisternas and Lam [11].

For a solution of n mixed electrolytes, the following mixing rules were proposed:

$$K_m = \sum_{i=1}^{n} Y_i K_i \tag{7}$$

$$\chi_m = \sum_{i=1}^{n} Y_i \chi_i \tag{8}$$

Table 1
SWVP correlations

Model	Validity	Accuracy	Refs.
$(P_{v,w} - P_{v,sw})/P_{v,w} = a \times Cl + b \times Cl^2$ $a = 9.2 \times 10^{-4}$ $b = 2.360 \times 10^{-6}$	$P_{v,w}$ = 3,167.2 Pa at 25°C; t_{48} = 25°C; 10 < Cl < 22%	±0.2%	Robinson [5]
$\log_{10}(P_{v,sw} - P_{v,w}) = a \times S_p - b \times S_p^2$ $a = -2.1609 \times 10^{-4}$ $b = 3.5012 \times 10^{-7}$	100 < t_{48} < 180°C; 35 < S_p < 170 g/kg	±0.07% with $P_{v,w}$ data from NEL steam Tables	Emerson and Jamieson [6]
$\ln(P_{v,sw}) = a - b \times (100/T_{48}) - c \ln(T_{48}/100) - d \times S_p$ a = 24.4543 b = 67.4509 c = 4.8489 $d = 5.44 \times 10^{-4}$	$P_{v,sw}$ in (atm); 273 < T_{48} < 313 K; 0 < S_p < 40 g/kg	±0.015%	Weiss and Price [7]
$P_{v,sw} = P_{v,w} + a \times S_p + b \times S_p^{3/2}$ $a = -2.3311 \times 10^{-3} - 1.4799 \times 10^{-4} t_{68} - 7.520 \times 10^{-6} t_{68}^2 - 5.5185 \times 10^{-8} t_{68}^3$ $b = -1.1320 \times 10^{-5} - 8.7086 \times 10^{-6} t_{68} + 7.4936 \times 10^{-7} t_{68}^2 - 2.6327 \times 10^{-8} t_{68}^3$	$P_{v,sw}$ and $P_{v,w}$ in (mm Hg); 0 < t_{68} < 40°C; 0 < S_p < 40 g/kg	±0.02% with $P_{v,w}$ data from Ambrose and Lawrenson	Millero [8]
$\ln(P_{v,sw}) = \frac{a+b\times T+c\times S+d\times T\times S}{1+e\times T+f\times S+g\times T\times S}$ $a = -4.541 \times 10^{-1}$; $b = 7.150 \times 10^{-2}$; $c = -3.159 \times 10^{-5}$; $d = -7.900 \times 10^{-5}$ $e = 4.303 \times 10^{-3}$; $f = -1.074 \times 10^{-3}$; $g = -4.620 \times 10^{-6}$	$P_{v,sw}$ in (kPa); 283 < t < 393°K; 35 < S_p < 170 g/kg	±0.07%	Valderrama and Campusano [4]
$\ln(P_{v,sw}) = \frac{a+b\times T+c\times S+d\times T\times S}{1+e\times T}$ $a = -4.483 \times 10^{-1}$; $b = 7.152 \times 10^{-2}$; $c = -6.580 \times 10^{-4}$; $d = -2.831 \times 10^{-6}$ $e = 4.303 \times 10^{-3}$	$P_{v,sw}$ in (kPa); 283 < t < 393°K; 35 < S_p < 170 g/kg	±0.1%	Valderrama and Campusano [4]

where K_i and χ_i are the values of these parameters for the single electrolyte solution containing only electrolyte i and Y_i is the ionic strength fraction of electrolyte i, which is calculated by dividing the ionic strength of electrolyte i by the total ionic strength of the mixture. In addition, if K is not available, then it can be estimated using an equation with two constants for each ion ($K = K_+ + K_- + \delta_+\delta_-$). The ion constant values for 23 cations and 31 anions were reported by Cisternas and Lam [11].

Cisternas and Lam [11] examined the model for 111 single and 37 mixed electrolyte systems up to 44 mol kg^{-1} of ionic strength. In addition, the model was applied to electrolyte mixtures with methanol, ethanol, isopropyl alcohol, isopentyl alcohol, acetonitrile, and water as solvents. This model has been applied in several studies: for example, Koronaki et al. [14] used the CL model to predict the humidity ratio of liquid desiccant with LiCl, LiBr, and $CaCl_2$ aqueous solutions; Moghaddam et al. [15] used the model to describe a small-scale, single-panel, liquid-to-air membrane energy exchanger; and Valia et al. [16] used the model to describe the fluid flow and heat and mass transfer in a counter-cross-flow liquid-to-air membrane energy exchanger. In all these cases, the results were satisfactory.

3. Prediction of SWVP using the CL model

The CL model can be applied to the prediction or correlation of the SWVP because the CL model can be applied to aqueous electrolytes mixtures. The sea water can be considered an aqueous mixture of electrolytes. Two sets of experimental data are used to study the capabilities of prediction of the CL model. The first set of data was given by Higashi et al. [17] and considers 128 SWVP data points ranging from 0 to 175°C and salinities ranging from 18.07 to 289.05 g kg^{-1}. Here, this set of experimental data is named Higashi. The second set of experimental data was given by Arons et al. [18], with 165 SWVP experimental data points ranging from −10 to 35°C and salinities ranging from 9.03 to 289.05 g kg^{-1}. This data-set is named Arons.

The CL model can be applied to mixed electrolytes using Eqs. (7) and (8). The ion relative concentration in sea water is almost constant, and the ionic strength fraction is thus also almost constant. The ionic strength can be calculated using the following equation: $I = 0.019915\,S_p/(1 - 1.00487 \times 10^{-3}\,S_p)$, where S_p is the salinity, expressed as g kg^{-1}. The water constants are as follows: $A_s = -0.021302$, $B_s = -5.390915$, $C_s = 7.192959$, $D_s = 1{,}730.2857$, and $E_s = 39.53$. However, the concentrations must be based on the electrolyte concentration and not on the ion concentration. Therefore, the sea water concentration must be expressed in terms of electrolytes. There are several ways to do so and, thus, several potential values for the K and χ. Table 2 shows two alternatives to represent the sea water concentration. The compositions of sea water components, based on the sea water mineralization, were compared with the values given by Millero et al. [19]. The mineralization 1 showed a mean absolute deviation of 0.0004 and a maximum deviation of 0.0013 mol fraction. The mineralization 2 showed a mean absolute deviation of 0.0008 and a maximum deviation of 0.0017 mol fraction. The K values obtained in both alternatives are similar, with values of 0.32192 and 0.32443 for alternatives 1 and 2, respectively. The first alternative was developed considering that the main cations in sea water are Na^+, M^{2+}, Ca^{2+}, K^+, and Sr^{2+} and that the main anions are Cl^-, SO_4^{2-}, and CO_3^{2-} (this also include HCO_3^-) [20], and it uses the K values that are available in CL [10]. The second alternative was developed based on the usual mineralization given for sea water [21]. However, in this case, the K values for $CaCO_3$ and $CaSO_4$ electrolytes were not available, so these K values were estimated based on the equation $K = K_+ + K_- + \delta_+\delta_-$.

To compare the experimental and calculated SWVP, the average ($\bar{e}$) and maximum error (max e) were calculated using the following equation:

Table 2
Two alternatives of sea water mineralization

Sea water mineralization 1		Sea water mineralization 2	
Ionic Strength fraction			
Na_2CO_3	0.0043	NaCl	0.6663
NaCl	0.8592	$MgCl_2$	0.1718
$CaCl_2$	0.0189	$MgSO_4$	0.0790
KCl	0.0184	$CaSO_4$	0.0530
$MgSO_4$	0.0521	K_2SO_4	0.0212
$MgCl_2$	0.0468	$CaCO_3$	0.0069
$SrCl_2$	0.0003	$MgBr_2$	0.0019
Total	1	Total	1
K	0.32192	K	0.32443
χ	1.59629	χ	1.59693
Higashi data-set			
$\bar{e}$	1.665	$\bar{e}$	1.696
max e	7.620	max e	7.744
Arons data-set			
$\bar{e}$	2.055	$\bar{e}$	2.084
max e	8.983	max e	9.109

$$e_k = 100 \times \left| \frac{P_k^{exp} - P_k^{cal}}{P_k^{exp}} \right| \quad (9)$$

where e_k is the error of data point k and P_k^{exp} and P_k^{cal} are the experimental and calculated SWVP. The results are given in Table 2. The average error for the Higashi and Arons data-sets is approximately 1.7 and 2.0%, respectively, and a maximum error of 7.7 and 9.1% was observed for Higashi and Arons data-sets, respectively. Better results are obtained for a small range of temperature and salinity. For example, the average error for the Higashi data-set from 273.15 to 448.15 K and 18.07 to 289.05 salinity is approximately 0.8%, with a maximum error of 2.8%. The same is observed for the Arons data-set: for temperatures between 263.15 and 308.15 K and salinity between 9.03 and 289.05 g kg^{-1}, the average error is approximately 1.0%, and the maximum error is 3.0%. In conclusion, the CL model can be used to predict the vapor pressure of sea water by representing the ionic concentration using an electrolyte concentration, with an average error of 1.87%.

4. Correlation of SWVP using the CL model

The CL model can be used to correlate the SWVP by assuming that the sea water is an aqueous solution of a pseudo 1:1 electrolyte; this model is based on equations 1 to 6, with $\chi = 2$. The K values are obtained by fitting the CL model to the experimental SWVP. For the Higashi and Arons experimental data-sets, K values of 0.03664 and 0.04702 were obtained, respectively. The average and maximum error for both data-sets are approximately 0.77 and 2.6%, respectively (see supplementary material for more details).

Tables 3 and 4 give the parameters adjusted for the CL model and the models given in Table 1 for the Higashi and Arons data-sets, respectively. For the Higashi data-set, the best results for both the average and maximum errors are obtained using the CL model; in addition, good results are observed for the Millero model [8]. In contrast, for the Arons data-set, the best results for both the average and maximum errors are found for the Millero model, and the CL model obtained the second-best results. Two interesting observation are as follows: (1) the CL model requires only one adjusted parameter, whereas the Millero model requires eight parameters to be adjusted; (2) the CL model gives very similar average and maximum errors for both experimental data-sets. Each model has a range of temperature and salinity (see Table 1) where it can be applied, and these ranges were not respected in this study. Fig. 1 compares the experimental data with the results given by the CL model.

5. Interpolation and extrapolation with the CL model

The capabilities in interpolation and extrapolation of the CL model were studied and compared with the other SWVP models. These studies are important because they provide information on the robustness of the model; this is the capability to represent SWVP at different conditions (temperature and salinity) from those used in the model fitting. The same experimental data-sets were used.

Table 3
Correlation of SWVP using the Higashi data-set

	Models						
Parameters	Cisternas and Lam	Robinson	Emerson and Jamieson	Weiss and Price	Valderrama and Campusano 4.1	Valderrama and Campusano 4.3	Millero
a	3.664×10^{-2}	5.591×10^{-4}	-4.235×10^{-9}	$1.738 \times 10^{+2}$	-5.134×10^{-1}	-5.042×10^{-1}	1.176×10^{-5}
b	–	5.903×10^{-6}	-1.526×10^{-6}	$-4.810 \times 10^{+2}$	7.07×10^{-2}	7.095×10^{-2}	-7.257×10^{-5}
c	–	–	–	$-1.168 \times 10^{+2}$	-7.004×10^{-4}	$-3.499E \times 10^{-5}$	2.024×10^{-7}
d	–	–	–	-9.730×10^{-4}	-2.831×10^{-6}	-7.954×10^{-5}	-2.062×10^{-9}
e	–	–	–	–	4.250×10^{-3}	4.256×10^{-3}	-3.067×10^{-5}
f	–	–	–	–	–	-1.054×10^{-3}	-3.507×10^{-6}
g	–	–	–	–	–	-4.620×10^{-6}	2.824×10^{-7}
h	–	–	–	–	–	–	-7.217×10^{-9}
$\bar{e}$	0.785	0.923	1.356	2.169	2.473	1.623	0.779
max e	2.311	3.507	5.003	7.185	8.330	4.092	5.162

Table 4
Correlation of SWVP using the Arons data-set

	Model						
Parameters	Cisternas and Lam	Robinson	Emerson and Jamieson	Weiss and Price	Valderrama and Campusano 4.1	Valderrama and Campusano 4.3	Millero
a	4.702×10^{-2}	6.229×10^{-4}	-4.317×10^{-9}	$1.867 \times 10^{+1}$	-5.481×10^{-1}	-5.179×10^{-1}	-5.980×10^{-5}
b	–	2.803×10^{-6}	-1.582×10^{-6}	$-5.268 \times 10^{+1}$	7.149×10^{-2}	7.149×10^{-2}	-1.316×10^{-5}
c	–	–	–	3.773×10^{-1}	-6.609×10^{-4}	-3.232×10^{-5}	1.606×10^{-6}
d	–	–	–	-1.012×10^{-3}	-2.896×10^{-6}	-7.903×10^{-5}	-6.138×10^{-8}
e	–	–	–	–	4.303×10^{-3}	4.174×10^{-3}	-2.599×10^{-5}
f	–	–	–	–	–	-1.037×10^{-3}	-1.349×10^{-6}
g	–	–	–	–	–	-4.812×10^{-6}	-1.805×10^{-7}
h	–	–	–	–	–	–	1.735×10^{-9}
$\bar{e}$	0.760	2.057	1.388	1.495	3.905	1.805	0.404
max *e*	2.887	4.812	2.807	5.096	7.820	4.274	2.882

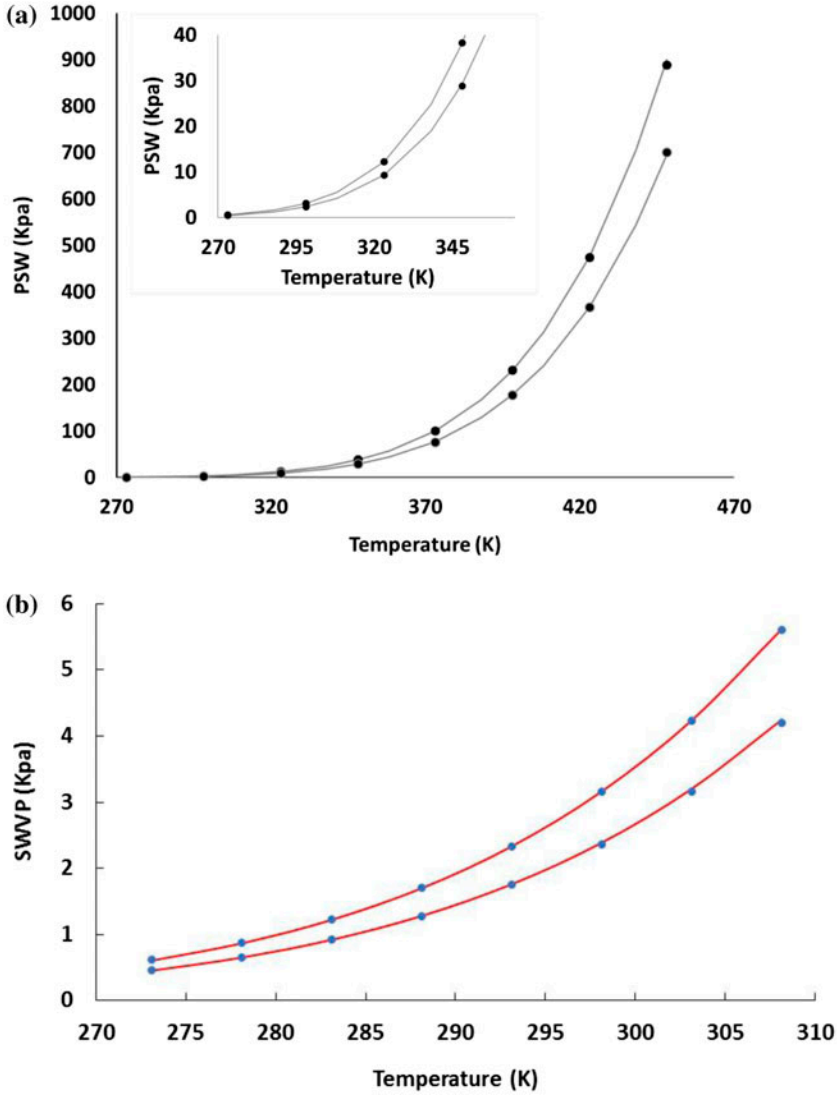

Fig. 1. Experimental (points) and correlated (line) SWVP using CL model: (a) at salinities of (from bottom to top) 18.07 and 289.05 g kg^{-1} (Higashi data-set) and (b) at salinities of (from bottom to top) 9.03 and 289.05 g kg^{-1} (Arons data-set).

Table 5
Interpolation of SWVP using the Higashi data-set

Parameters	Model						
	Cisternas and Lam	Robinson	Emerson and Jamieson	Weiss and Price	Valderrama and Campusano 4.1	Valderrama and Campusano 4.3	Millero
a	4.198×10^{-2}	5.557×10^{-4}	2.112×10^{-5}	$1.705 \times 10^{+2}$	-5.031×10^{-1}	-5.018×10^{-1}	-1.462×10^{-6}
b	–	5.768×10^{-6}	-1.526×10^{-6}	$-4.745 \times 10^{+2}$	7.052×10^{-2}	7.101×10^{-2}	-7.053×10^{-5}
c	–	–	–	$-1.140 \times 10^{+2}$	-8.205×10^{-4}	-8.805×10^{-5}	4.461×10^{-8}
d	–	–	–	-9.771×10^{-4}	-2.831×10^{-6}	-7.904×10^{-5}	-2.062×10^{-9}
e	–	–	–	–	4.224×10^{-3}	4.260×10^{-3}	-3.070×10^{-5}
f	–	–	–	–	–	-1.062×10^{-3}	-2.677×10^{-6}
g	–	–	–	–	–	-4.620×10^{-6}	2.824×10^{-7}
h	–	–	–	–	–	–	-7.217×10^{-9}
$\bar{e}$	0.805	0.872	1.238	2.127	3.015	1.529	0.994
max e	1.341	2.733	3.658	3.534	4.666	3.109	5.079
$\bar{e}$ (inter)	0.781	0.940	1.660	3.467	2.541	1.076	0.877
max e (inter)	2.055	3.068	3.564	8.143	5.412	3.015	5.986

Table 6
Interpolation of SWVP using the Arons data-set

Parameters	Models						
	Cisternas and Lam	Robinson	Emerson and Jamieson	Weiss and Price	Valderrama and Campusano 4.1	Valderrama and Campusano 4.3	Millero
a	4.137×10^{-2}	6.587×10^{-4}	1.123×10^{-5}	$1.862 \times 10^{+1}$	-5.584×10^{-1}	-5.257×10^{-1}	-6.284×10^{-5}
b	–	4.711×10^{-6}	-1.582×10^{-6}	$-5.254 \times 10^{+1}$	7.141×10^{-2}	7.145×10^{-2}	-1.316×10^{-5}
c	–	–	–	3.786×10^{-1}	-7.442×10^{-4}	-5.681×10^{-5}	1.589×10^{-6}
d	–	–	–	-1.075×10^{-3}	-3.298×10^{-6}	-7.917×10^{-5}	-6.138×10^{-8}
e	–	–	–	–	2.059×10^{-3}	3.144×10^{-3}	-2.589×10^{-5}
f	–	–	–	–	–	-1.093×10^{-3}	-1.349×10^{-6}
g	–	–	–	–	–	-2.901×10^{-6}	-1.805×10^{-7}
h	–	–	–	–	–	–	1.735×10^{-9}
$\bar{e}$	1.155	2.444	1.062	2.099	6.610	4.313	0.729
max e	2.766	5.006	2.984	3.521	15.663	8.411	2.661
$\bar{e}$ (inter)	0.749	4.779	1.514	1.980	4.978	3.207	0.395
max e (inter)	2.738	5.249	3.109	3.878	14.439	8.225	1.841

For the interpolation study, the Higashi data at temperatures of 273.15, 373.15, and 448.15 K and salinities of 18.07, 144.52, and 289.05 g kg^{-1} were used to fit the parameters models. Next, the models were used to predict (interpolate) SWVP at temperatures of 298.15, 323.15, 348.15, 398.15, and 423.15 K and salinities of 36.13, 54.20, 72.26, 90.33, 108.39, 126.46, 162.59, 180.66, 198.72, 216.79, 234.85, 252.92, and 270.98 g kg^{-1}. Similarly, the Arons data at temperatures of 263.15, 283.15, and 308.15 K and salinities of 9.03, 144.52, and 289.05 g kg^{-1} were used to fit the parameters models. Next, the models were used to predict (interpolate) SWVP at temperatures of 273.15, 278.15, 288.15, 293.15, 298.15, and 303.15 K and salinities of 18.07, 36.13, 54.20, 72.26, 90.33, 108.39, 126.46, 162.59, 180.66, 198.72, 216.79, 234.85, 252.92, and 270.98 g kg^{-1}. The results are given in Tables 5 and 6 for the Higashi and Arons data-sets, respectively. The best results for both the correlated and interpolated data of the Higashi data-set were obtained with the CL model, followed by the Millero model. In addition, good results were observed for the Robinson model [5]; however, this model requires the experimental values of water vapor pressure at the temperature of evaluation. For the Arons data-set, the opposite was observed: the best results were obtained for the Millero model, followed

Table 7
Extrapolation of SWVP using the Higashi data-set

	Models						
Parameters	Cisternas and Lam	Robinson	Emerson and Jamieson	Weiss and Price	Valderrama and Campusano 4.1	Valderrama and Campusano 4.3	Millero
a	-1.102×10^{-3}	5.910×10^{-4}	-4.128×10^{-6}	$1.629 \times 10^{+2}$	-4.643×10^{-1}	-4.901×10^{-1}	1.466×10^{-4}
b	–	5.903×10^{-6}	-1.694×10^{-6}	$-4.551 \times 10^{+2}$	7.055×10^{-2}	7.103×10^{-2}	-6.668×10^{-5}
c	–	–	–	$-1.084 \times 10^{+2}$	-8.547×10^{-4}	-9.944×10^{-5}	4.461×10^{-8}
d	–	–	–	-9.719×10^{-4}	-2.831×10^{-6}	-7.894×10^{-5}	-2.062×10^{-9}
e	–	–	–	–	4.203×10^{-3}	4.256×10^{-3}	-4.734×10^{-5}
f	–	–	–	–	–	-1.060×10^{-3}	-2.677×10^{-6}
g	–	–	–	–	–	-4.620×10^{-6}	2.824×10^{-7}
h	–	–	–	–	–	–	-7.217×10^{-9}
$\bar{e}$	0.714	0.636	1.071	0.478	0.654	0.352	0.749
max e	1.451	1.571	3.121	1.630	2.015	0.805	1.441
$\bar{e}$ (extra)	0.940	1.028	2.176	5.265	2.436	1.250	1.353
max e (extra)	4.142	4.095	8.281	20.545	8.328	4.291	8.354

Table 8
Extrapolation of SWVP using the Arons data-set

	Models						
Parameters	Cisternas and Lam	Robinson	Emerson and Jamieson	Weiss and Price	Valderrama and Campusano 4.1	Valderrama and Campusano 4.3	Millero
a	2.443×10^{-2}	4.347×10^{-4}	5.668×10^{-6}	$1.866 \times 10^{+1}$	-4.998×10^{-1}	-4.992×10^{-1}	-4.137×10^{-5}
b	–	2.546×10^{-6}	-1.822×10^{-6}	$-5.265 \times 10^{+1}$	7.126×10^{-2}	7.137×10^{-2}	-1.327×10^{-5}
c	–	–	–	3.880×10^{-1}	-7.484×10^{-4}	-5.705×10^{-5}	1.589×10^{-6}
d	–	–	–	-9.226×10^{-4}	-3.864×10^{-6}	-7.948×10^{-5}	-6.138×10^{-8}
e	–	–	–	–	3.382×10^{-3}	4.195×10^{-3}	-2.567×10^{-5}
f	–	–	–	–	–	-1.050×10^{-3}	-1.349×10^{-6}
g	–	–	–	–	–	-4.792×10^{-6}	-1.805×10^{-7}
h	–	–	–	–	–	–	1.735×10^{-9}
$\bar{e}$	0.359	1.683	1.274	0.420	1.236	0.693	0.227
max e	1.139	3.205	2.812	1.266	3.183	1.598	0.598
$\bar{e}$ (extra)	0.992	3.122	2.275	2.412	3.671	1.693	0.628
max e (extra)	2.900	9.322	6.175	8.473	12.921	5.296	4.257

by the CL model. The Emerson and Jamieson model [6] also gave good results, but similar to the Robinson model, the experimental value of water vapor pressure is required.

For the extrapolation study, data from Higashi at temperatures of 323.15, 348.15, 373.15, and 398.15 K and salinities of 72.26, 90.33, 108.39, 126.36, 144.52, 162.59, 180.66, 198.72, and 216.79 g kg^{-1} were used to fit the parameter models. Next, the models were used to predict (extrapolate) the SWVP at temperatures of 273.15, 298.15, 423.15, and 448.15 K and salinities of 18.07, 36.13, 54.20, 234.85, 252.92, 270.98, and 289.05 g kg^{-1}. In an analogous manner, data from Aron at temperatures of 278.15, 283.15, 288.15, and 293.15 K and salinities of 72.26, 90.33, 108.39, 126.46, 144.52, 162.59, 180.66, 198.72, and 216.79 g kg^{-1} were used to fit the parameter models. Next, the models were used to predict (extrapolate) the SWVP at temperatures of 263.15, 268.15, 273.15, 298.15, and 303.15 K and salinities of 9.03, 18.07, 36.13, 54.20, 234.85, 252.92, 270.98, and 289.05 g kg^{-1}. The results are given in Tables 7 and 8 for the Higashi and Arons data-sets, respectively. Several models are found to provide good results in the correlation of the

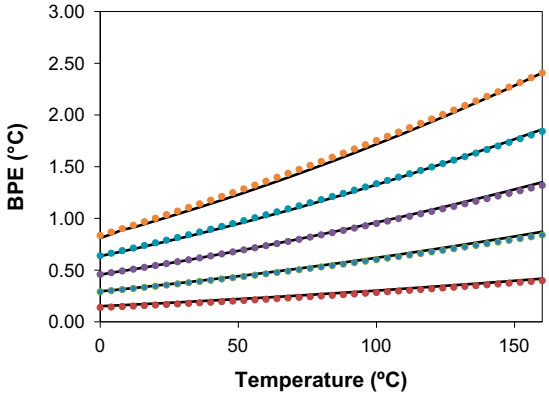

Fig. 2. BPE calculated using the Cisternas–Lam model with $K = 0.03664$ (lines) and Fabuss–Korosi model (points) at salinities of (from bottom to top) 20, 40, 60, 80, and 100 g kg^{-1}.

experimental SWVP. Indeed, for the Higashi data-set, the Valderrama and Campusano 4.3, Weiss and Price [7], Robinson, Valderrama and Campusano 4.1, CL, and Millero models gave average errors of 0.35, 0.48, 0.64, 0.65, 0.71, and 0.75%, respectively. However, the prediction (extrapolation) average error for the CL, Robinson, Valderrama and Campusano 4.3, Millero, Valderrama and Campusano 4.1, and Weiss and Price models was 0.94, 1.03, 1.25, 1.35, 2.44, and 5.27%, respectively. In addition, the maximum error in the extrapolation was over 8% for all models, with the exception of the Robinson, CL, and Valderrama and Campusano 4.3 models, which gave values of 4.10, 4.14, and 4.29%, respectively. For the Arons data-set, the models of Millero, CL, Weiss and Price, and Valderrama and Campusano 4.3 gave correlation average errors of 0.28, 0.36, 0.42, and 0.69%, respectively. However, for the extrapolation, only the Millero and CL models gave average error values below 1%. Again, the maximum extrapolation error were high for almost all of the models, with the CL and Millero models having acceptable values (2.90 and 4.26% for the CL and Millero models, respectively).

6. Prediction of the BPE using the CL model

The boiling temperature of sea water is higher than that of pure water at a given pressure by an amount named the BPE because increasing the salinity of sea water lowers the vapor pressure. The vapor pressure and boiling temperature can be obtained from each other by inverting the boiling temperature function and the vapor pressure function, respectively. Therefore, the CL model can also be used to estimate the BPE. Using the same K value used for vapor pressure ($K = 0.03664$), the CL model was applied to predict the BPE of sea water solutions. The values were compared with the values given by the Fabuss and Korosi [22] model. The Fabuss and Korosi model is valid for $0 \le t \le 200$ °C and salinity from 0 to 120 g kg^{-1}, with an accuracy of 0.018 K [1]. The results are shown in Fig. 2; the accuracy of CL model compared with the Fabuss and Korosi model is 0.015 K.

7. Conclusions

In conclusion, the CL model can be used to predict the vapor pressure of sea water by representing the ionic concentration using electrolyte concentration, with an average error of 1.87%. In addition, the CL model can be used to correlate the SWVP with an average error of 0.77% using the parameter K as a fitting parameter and by considering the sea water to be a pseudo 1:1 electrolyte. Only the Millero model gives similar results for SWVP correlation, but it requires eight fitting parameters. On average, the best results for prediction (interpolation and extrapolation) of SWVP are obtained using the CL model. The Millero model also gives good average errors, but the maximum error is approximately two times the value of the CL model. The CL model can also be used to predict the BPE with good accuracy.

Supplementary material

The supplemental material for this paper is available online at http://dx.doi.org/10.1080/19443994.2015.1135481.

Acknowledgments

L.A.C. thanks CONICYT and the Regional Government of Antofagasta for their funding through the PAI program, Project Anillo ACT 1,201. R.A. thanks CICITEM (R10C1004) and the Antofagasta Regional Government.

References

[1] M.H. Sharqawy, J.H.V. Lienhard, S.M. Zubair, Thermophysical properties of seawater: A review of existing correlations and data, Desalin. Water Treat. 16 (2010) 354–380.
[2] J.O. Valderrama, R.A. Campusano and A.S. Toro, Correlation and prediction of saline solution properties for their use in mineral processing using artificial neural networks, J. Water Reuse Desalin. 5 (2015) 454–464.
[3] J.V. Tu, Advantages and disadvantages of using artificial neural networks versus logistic regression for predicting medical outcomes, J. Clin. Epidemiol. 49 (1996) 1225–1231.

[4] J.O. Valderrama, R.A. Campusano, Physicochemical, transport and thermodynamic properties of saline solutions for process design using Pade´ approximants, Desalin. Water Treat. (2015), doi: 10.1080/19443994.2015.1022806.
[5] R.A. Robinson, The vapour pressure and osmotic equivalence of sea water, J. Mar. Biol. Assoc. U.K. 33 (1954) 449–455.
[6] W.H. Emerson, D.T. Jamieson, Some physical properties of sea water in various concentrations, Desalination 3 (1967) 213–224.
[7] R.F. Weiss, B.A. Price, Nitrous oxide solubility in water and seawater, Mar. Chem. 8 (1980) 347–359.
[8] F.J. Millero, The thermodynamics of seawater. Part II; Thermochemical properties, Ocean Sci. Eng. 8 (1983) 1–40.
[9] R. Feistel, A Gibbs function for seawater thermodynamics for −6 to 80˚C and salinity up to 120 g kg^{-1}, Deep Sea Res. Part I: Oceanogr. Res. Pap. 55 (2008) 1639–1671.
[10] L.A. Cisternas, E.J. Lam, A analytic correlation of vapour pressure of aqueous and non-aqueous solutions of single and mixed electrolytes, Fluid Phase Equilib. 53 (1989) 243–249.
[11] L.A. Cisternas, E.J. Lam, An analytic correlation for the vapour pressure of aqueous and non-aqueous solutions of single and mixed electrolytes. Part II. Application and extension, Fluid Phase Equilib. 62 (1991) 11–27.
[12] A. Kumar, V.S. Patwardhan, Prediction of vapour pressure of aqueous solutions of single and mixed electrolytes, Can. J. Chem. Eng. 64 (1986) 831–838.
[13] V.S. Patwardhan, A. Kumar, A unified approach for prediction of thermodynamic properties of aqueous mixed-electrolyte solutions. Part I. Vapor pressure and heat of vaporization, AIChE J. 32 (1986) 1419–1428.
[14] I.P. Koronaki, R.I. Christodoulaki, V.D. Papaefthimiou, E.D. Rogdakis, Thermodynamic analysis of a counter flow adiabatic dehumidifier with different liquid desiccant materials, Appl. Therm. Eng. 50 (2013) 361–373.
[15] D.G. Moghaddam, A. Oghabi, G. Ge, R.W. Besant, C.J. Simonson, Numerical model of a small-scale liquid-to-air membrane energy exchanger: Parametric study of membrane resistance and air side convective heat transfer coefficient, Appl. Therm. Eng. 61 (2013) 245–258.
[16] A. Vali, G. Ge, R.W. Besant, C.J. Simonson, Numerical modeling of fluid flow and coupled heat and mass transfer in a counter-cross-flow parallel-plate liquid-to-air membrane energy exchanger, Int. J. Heat Mass Transf. 89 (2015) 1258–1276.
[17] K. Higashi, K. Nakamura, R. Hara, The specific gravities and the vapor pressure of the concentrated sea water at 0–175˚C, J. Soc. Chem. Ind. Japan 34 (1931) 166–172.
[18] A.B. Arons, C.F. Kientzler, Vapor pressure of sea-salt solutions, Trans., Am. Geophys. Union 35 (1954) 722–728.
[19] F.J. Millero, R. Feistel, D.G. Wright, T.J. McDougall, The composition of standard seawater and the definition of the reference-composition salinity scale, Deep Sea Res. Part I: Oceanogr. Res. Pap. 55 (2008) 50–72.
[20] E. Brown, A. Colling, D. Park, J. Phillips, D. Rothery, J. Wright, Seawater: Its Composition, Properties and Behavior, second ed., Elsevier Science Ltd, Kidlington, 1995.
[21] J. Valderrama, L. Cisternas, E. Gálvez, Propiedades fisicoquímica del agua de mar para procesos industriales (Physico-chemical properties of sea water for industrial processes) (in Spanish), in: L. Cisternas, L. Moreno, El agua de mar en la minería (Seawater in mining), Master Ril, Santiago, 2014.
[22] B.M. Fabuss, A. Korosi, Boiling point elevation of sea water and its concentrates, J. Chem. Eng. 11 (1966) 606–609.